Sensors and Actuators B 216 (2015) 467–475

Contents lists available at ScienceDirect

Sensors and Actuators B: Chemical

journal homepage: www.elsevier.com/locate/snb

Flexible humidity sensor based on Au nanoparticles/graphene oxide/thiolated silica sol–gel film

Pi-Guey Su*, Wei-Luen Shiu, Meng-Shian Tsai

Department of Chemistry, Chinese Culture University, Taipei 111, Taiwan

ARTICLE INFO

Article history:
Received 18 January 2015
Received in revised form 10 April 2015
Accepted 22 April 2015
Available online 28 April 2015

Keywords:
Self-assembly
Sol–gel
Flexible humidity sensor
Graphene oxide
Gold nanoparticles

ABSTRACT

Novel flexible impedance-type humidity sensors that were based on gold nanoparticles (AuNPs) and graphene oxide (GO) were fabricated by a combination of self-assembly and the sol–gel technique. A hydrolyzed 3-mercaptopropyltrimethoxysilane (MPTMOS) sol–gel solution that contained GO was firstly dropped on to the surface of a pair of comb-like Au electrodes on a polyethylene terephthalate (PET) substrate, and then AuNPs were assembled onto the thiol groups of the sol–gel network. The formed AuNPs were characterized by UV–vis spectroscopy. The microstructure of the AuNPs/GO/MPTMOS sol–gel film was analyzed by atomic force microscope (AFM) and scanning electron microscopy (SEM). The effects of the AuNPs and the amount of GO added on the flexibility, electrical and humidity sensing properties of the AuNPs/GO/MPTMOS sol–gel films on a PET substrate were investigated. The sensor that was made from the AuNPs/GO/MPTMOS sol–gel film with 9.0 wt% added GO exhibited the greatest flexibility, sensitivity, linearity and long-term stability. The effects of applied frequency, ambient temperature, response and recovery times on the impedance of the flexible humidity sensor were also investigated. The sensing mechanism of the AuNPs/GO/MPTMOS sol–gel film was explained with reference to impedance plots.

1. Introduction

Today, flexible electronic devices are attracting much interest, owing to the proliferation of handheld portable consumer electronics. A new trend towards the direct integration of sensors on flexible systems with various functions has become evident. For multifunction applications, flexible multisensor platforms should be manufactured at very low-cost, low energy consumption, easy-fabrication and integrated into smart systems. Inorganic nanomaterials are more attractive than flexible organic electronic sensors for the development of flexible chemical sensors because they can be prepared under ambient conditions and they exhibit high carrier mobility, tunable porosity, high thermal stability and high chemical inertness [1,2].

The sol–gel process is a low-temperature method for the preparation of a three-dimensional network of inorganic materials that involves the hydrolysis and condensation of silicon alkoxides precursors [1,3–5]. Self-assembly has become a popular surface derivatization method for preparing modified surfaces with desired properties because of its simplicity, low-cost, low temperature of deposition, and the controllable thickness (from nanometers to micrometers), high degree of organization and homogeneity of the prepared product [4,6,7]. Therefore, the sol–gel process and self-assembly can be combined to provide a fast, simple and more effective method for fabricating biosensors [1,8,9]. Liang et al. fabricated a hepatitis B surface antigen (HBsAg) immunosensor that was made by the self-assembly of gold nanoparticles and hepatitis B surface antibody (HBsAb) on a 3-mercaptopropyltrimethoxysilane (MPTMOS) sol–gel network-modified gold electrode [1]. Norooz-ifar et al. fabricated an electrochemical cyanide sensor that was made by the self-assembly of Ag nanoparticles (AgNPs) on an MPTMOS sol–gel network-modified gold electrode [8]. Wu et al. fabricated an amperometric acetylcholine biosensor by the self-assembly of Au nanoparticles (AuNPs) and acetylcholinesterase on the sol–gel/multi-walled carbon nanotubes/choline oxidase composite-modified platinum electrode [9]. Notably, in these studies, sol–gel-derived inorganic materials were deposited on rigid substrates.

AuNPs have attracted much interest because of their attractive electronic and unique optical, thermal and physical properties, their large surface area, their catalytic activity and their potential

* Corresponding author. Tel.: +886 2 28610511x25332; fax: +886 2 28614212.
E-mail addresses: spg@faculty.pccu.edu.tw, spg@ulive.pccu.edu.tw (P.-G. Su).

http://dx.doi.org/10.1016/j.snb.2015.04.070
0925-4005/

usefulness in chemical sensors and biosensors [10]. Additionally, graphene is crucial to many sensing devices owing to its high mechanical strength, flexibility, surface area, carrier mobility and electron transfer at room temperature, as well as its low manufacturing cost [11–13]. The oxidation of graphite using strongly acidic oxidants [14] yields graphene oxide (GO) with hydroxyl and epoxide functional groups on their basal planes and carboxyl groups at the sheet edges [15]. These groups are responsible for the high hydrophilicity and electrical insulation of GO. This GO, which can be reduced using various reductants such as hydrazine, sodium borohydride and ascorbic acid [16–18], greatly increasing the electrical conductivity of the reduced GO [19,20].

Humidity sensors are widely used in measurement and control of humidity in human comfort and a myriad of industrial processes. Therefore, there has been increasing the important of accurate, precise measurement of humidity. Additionally, designing a high-performance humidity sensor must meet many requirements, including linear response, high sensitivity, fast response time, chemical and physical stability, wide operating range of humidity and low cost. Recently, many groups have used GO and reduced GO sensing materials to detect humidity [21–24]. Yao et al. fabricated a humidity sensor by spin-coating chemically derived graphene oxide on a quartz crystal microbalance (QCM) [21]. Sun et al. fabricated a flexible humidity sensor by spin-coating GO film on PET substrate and then reducing the GO film using two-beam-laser interference (TBLI) [22]. Zeng et al. fabricated a humidity sensor by drop-coating defective graphene on alumina substrate [23]. Chen et al. fabricated a stress-type humidity sensor that was based on a graphene oxide-silicon bi-layer flexible structure [24]. However, no attempt has been made to fabricate flexible humidity sensors that are based on hydrolyzed three-dimensional sol–gel network inorganic materials. In this work, AuNPs/GO/MPTMOS sol–gel films are fabricated on a polyethylene terephthalate (PET) substrate to form flexible impedance-type humidity sensors by combining the sol–gel process and self-assembly. The films were characterized by atomic force microscopy (AFM), scanning electron microscopy (SEM) and UV-Vis spectrophotometer. The electrical characteristics of the AuNPs/GO/MPTMOS sol–gel films were studied as functions of RH. The effects of the AuNPs and the amount of GO added in the AuNPs/GO/MPTMOS sol–gel film on its electrical and humidity-sensing properties were investigated. The flexibility and humidity-sensing properties, including sensitivity, hysteresis, effects of applied frequency and ambient temperature, response time, recovery time and stability, were also investigated. Complex impedance spectra were obtained to elucidate the humidity-sensing mechanism of the AuNPs/GO/MPTMOS sol–gel film.

2. Experimental

2.1. Materials

The GO used in this work was prepared using Hummers method [14]. The purified GO was then dispersed in deionized water to form a 0.85 mg/mL suspension. Exfoliation of GO was achieved by using an ultrasonic bath. (3-mercaptopropyl)trimethoxy silane (MPTMOS, 95%), ethanol (99.8%) and hydrochloric acid (0.1 mol/L) were obtained from Aldrich. Sodium citrate was obtained from Shimakyu's Pure Chemicals. Hydrogen tetrachloroaurate(III) hydrate ($HAuCl_4{\cdot}xH_2O$, 99.9%) was obtained from UniRegion Bio-Tech. All reagents used were analytical grade. All used deionized water (DIW) was prepared using a Milli-Q Millipore (Bedford, MA, USA) purification system, and the resistivity of water was above 18.0 MΩ cm^{-1}.

2.2. Preparation of MPTMOS sol

Aqueous silica sol was prepared using the method in the literature [4]. Silica sol was prepared by mixing 1 mL MPTMOS, 0.8 mL ethanol, 4 mL water and 0.2 mL hydrochloric acid, and then sonicating this mixture for 30 min until a clear and homogeneous solution was obtained. This solution was stored at room temperature for 2–3 h.

2.3. Preparation of AuNPs

AuNPs was prepared using the method in the literature [25]. The AuNPs colloidal particles were prepared by adding 38.8 mM sodium citrate to boiling aqueous 1 mM $HAuCl_4$. The solution was boiled for 15 min with vigorous stirring, and then allowed to cool to room temperature, before being stored at 4 °C.

2.4. Fabrication of flexible humidity sensors

Fig. 1 schematically depicts the structure of the flexible humidity sensor. The interdigited Au electrodes were made on a flexible substrate (polyethylene terephthalate; PET) by sputtering initially Cr (thickness 50 nm) and then Au (thickness 250 nm) in a temperature range of 120–160 °C. The electrode gap was 0.2 mm. The substrates were firstly treated with an H_2O_2/H_2SO_4 mixture (1:2, 15 mL), washed in de-ionized water (DIW) and then cleaned in acetone solution for 3 min. Fig. 2 schematically depicts the fabrication of a flexible impedance-type humidity sensor using the sol–gel process, nanoparticles and self-assembly. First, a homogeneous stock GO/MPTMOS sol solution was prepared by carefully mixing 2 mL MPTMOS sol with the required amount of GO. Then, the fresh mixture was dropped on the PET substrate that contained a pair of interdigited Au electrodes, and allowed to dry at 4 °C. Finally, the GO/MPTMOS sol–gel was immersed in AuNPs solution for 5 h at 4 °C. A flexible impedance-type humidity sensor was thus obtained.

2.5. Instruments and analysis

The formation of AuNPs was characterized by UV–Vis spectroscopy (Agilent 8453). The surface microstructure of the thin film that was coated on a PET substrate was investigated using a field emission scanning electron microscope (FEI company, Nova NanoSEM^{TM} 230) equipped with an energy dispersive

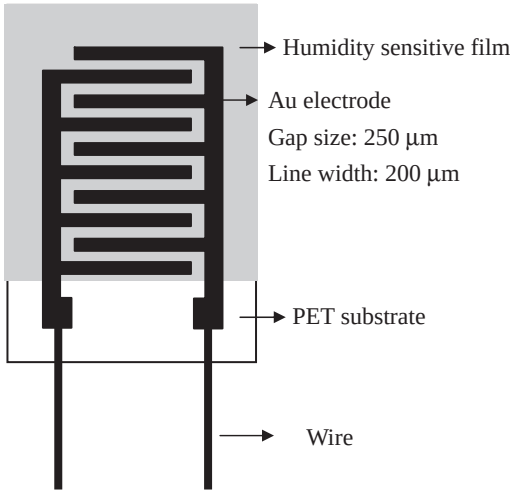

Fig. 1. Structure of humidity sensor.

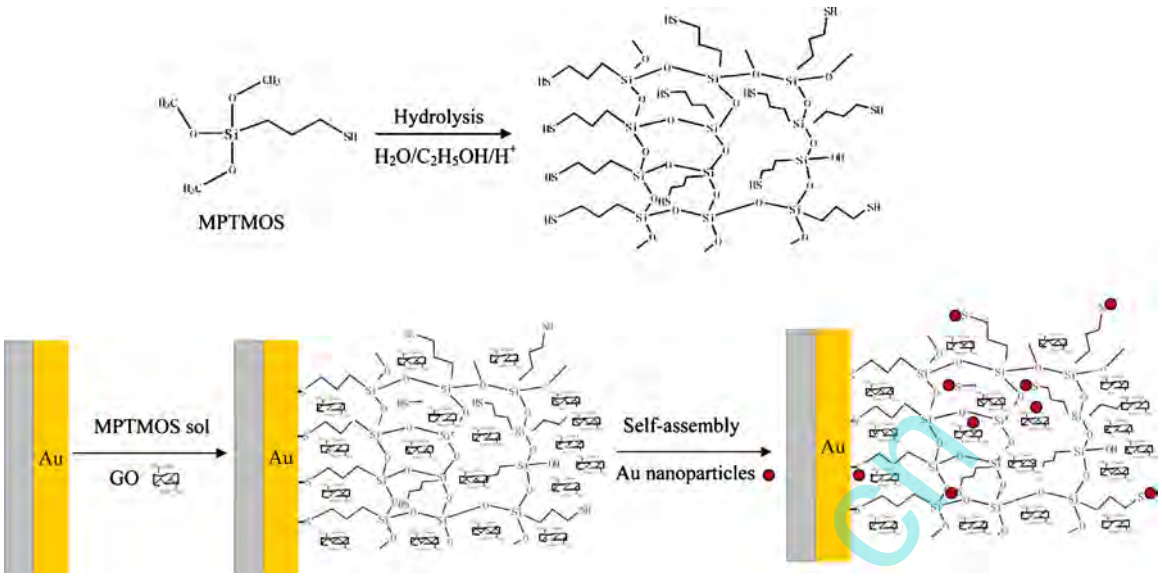

Fig. 2. Hydrolysis of MPTMOS and the fabrication of the flexible humidity sensor based on AuNPs/GO/MPTMOS sol–gel nano-hybride film by combining the sol–gel, nanoparticles and self-assembly technologies.

spectrometer (EDS) and an atomic force microscope (AFM, Ben-Yuan, CSPM 4000) in tapping mode which the horizontal and vertical resolution are 0.26 and 0.10 nm, respectively. The impedance of the sensor was measured as a function of RH using an LCR meter (Philips PM6306) in a test chamber under the conditions of a measurement frequency of 1 kHz, an applied voltage of 1 V, an ambient temperature of 25 °C. A frequency range of 50 Hz–100 kHz, an RH range from 20 to 90% at 25 °C and an applied voltage of 1 V were used in the complex impedance analysis. As shown in Fig. 3, a divided humidity generator was used as the principal facility for producing the testing gases. The required humidity was produced by adjusting the proportion of dry and humid air generated by the divided flow humidity generator under a total flow rate is 10 L/min. The model of two mass flow controller's (Hastings) and flow display power-supply used is the Protec PC-540 manufactured by Sierra Instruments Inc, as described elsewhere [26]. The RH values were measured using a calibrated hygrometer (Rotronic) with an accuracy of ±0.1% RH. Flexibility experiments were performed in which the sensor was bent to various degrees as their responses were monitored as a function of the period of exposure to humidity. The bending angle was measured using a goniometer.

3. Results and discussion

3.1. Preparation and characterization of AuNPs/GO/MPTMOS sol–gel films

Fig. 2 shows the process of fabrication of the flexible impedance-type humidity sensor that is based on the AuNPs/GO/MPTMOS sol–gel film. The MPTMOS sol contains two reactive functional groups, which were the trimethoxysilane head group and the thiol tail [27]. The trimethoxysilane head group can undergo hydrolysis and a condensation reaction to form a covalently linked siloxane network, which can be used to for encapsulate of MWCNTs. The thiol tail not only can be used to chemisorb onto the Au electrode surface but also can be used in the assembly of AuNPs by the formation of an Au–S bond. The AuNPs can be self-assembled both inside the network and on the surface of the MPTMOS sol–gel. AuNPs

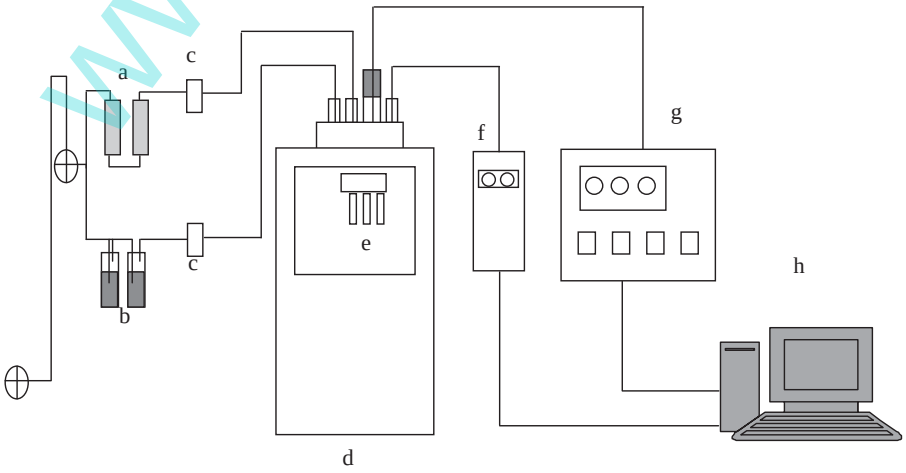

Fig. 3. Schematically plots the impedance measurement of sensors and the humidity atmosphere controller. (a) molecular sieve and desiccating agent; (b) water; (c) mass flow controller; (d) controlled temperature detection chamber; (e) humidity sensor; (f) hygrometer; (g) LCZ meter; (h) PC.

can act as tiny conduction centers and can facilitate the transfer of electrons [28].

3.1.1. Characteristics of as-prepared AuNPs and AuNPs/GO/MPTMOS sol–gel

Fig. 4 shows the UV–vis absorption spectra of as-prepared AuNPs and GO/MPTMOS sol–gel-encapsulated AuNPs. The absorption band of as-prepared AuNPs was obtained at about 520 nm. The absorption band of GO/MPTMOS sol–gel-encapsulated AuNPs (678 nm) was longer and broader than that of as-prepared AuNPs because that the AuNPs aggregated in the AuNPs/GO/MPTMOS sol–gel [29,30].

3.1.2. AFM and SEM analyses of microstructure of surface

The surface morphologies of the MPTMOS sol–gel, GO/MPTMOS sol–gel and AuNPs/GO/MPTMOS sol–gel films were investigated by AFM. Fig. 5 shows the AFM of the MPTMOS sol–gel, GO/MPTMOS sol–gel and AuNPs/GO/MPTMOS sol–gel on PET substrates. The root mean square (RMS) roughness of the MPTMOS sol–gel, GO/MPTMOS sol–gel and AuNPs/GO/MPTMOS sol–gel films was 1.27, 35.9 and 24.6 nm, respectively. The MPTMOS sol–gel film had a smooth surface because acid-catalyzed hydrolysis tends to yield many branched sols, which effectively support the cohesion of the film on a PET substrate [31] (Fig. 5(a)). The surfaces of both GO/MPTMOS sol–gel (Fig. 5(b)) and AuNPs/GO/MPTMOS sol–gel (Fig. 5(c)) were rougher than that of MPTMOS sol–gel. The GO/MPTMOS sol–gel exhibited a rough surface because the GO was immobilized in the MPTMOS sol–gel (Fig. 5(b)). Many bright particles clearly self-assembled on the outer surfaces of the AuNPs/GO/MPTMOS sol–gel film (Fig. 5(c)). FE-SEM images in Fig. 6 further reveal the surface morphologies of the GO/MPTMOS sol–gel and AuNPs/GO/MPTMOS sol–gel films. The 1.0 wt% GO/MPTMOS sol–gel film (Fig. 6(a)) exhibited a flat surface, and GO was incorporated into the 1.0 wt% GO/MPTMOS sol–gel film. When the amount of added GO was 9.0 wt%, the surface had an observed flakelike and wrinkled morphology (Fig. 6(b)). The high-magnification SEM image (inset in Fig. 6(b)) reveals that obviously naked GO was present on the surface of the 9.0 wt% GO/MPTMOS sol–gel film. The AuNPs/9.0 wt% GO/MPTMOS sol–gel film (Fig. 6(d)) had more particulate agglomerates than that of the AuNPs/1.0 wt% GO/MPTMOS sol–gel film (Fig. 6(c)). The high-magnification SEM image (inset in Fig. 6(d)) reveals obviously aggregated particles. The composition of the particles was determined by EDS, which yielded a spectrum that is presented in Fig. 6(e). The EDS analysis demonstrated that the AuNPs were surely self-assembled on GO/MPTMOS sol–gel film.

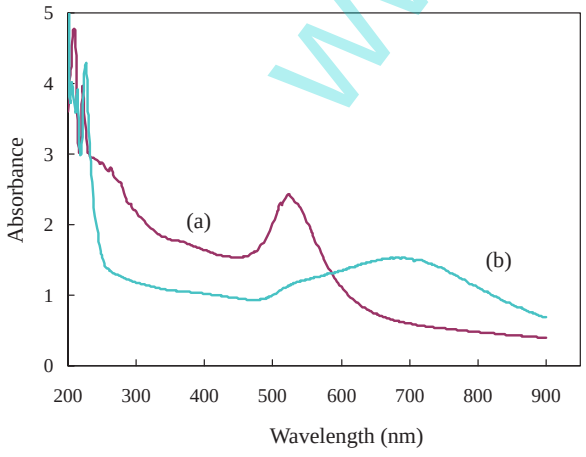

Fig. 4. UV–vis absorption spectra of (a) as-prepared AuNPs and (b) AuNPs/GO/MPTMOS sol–gel.

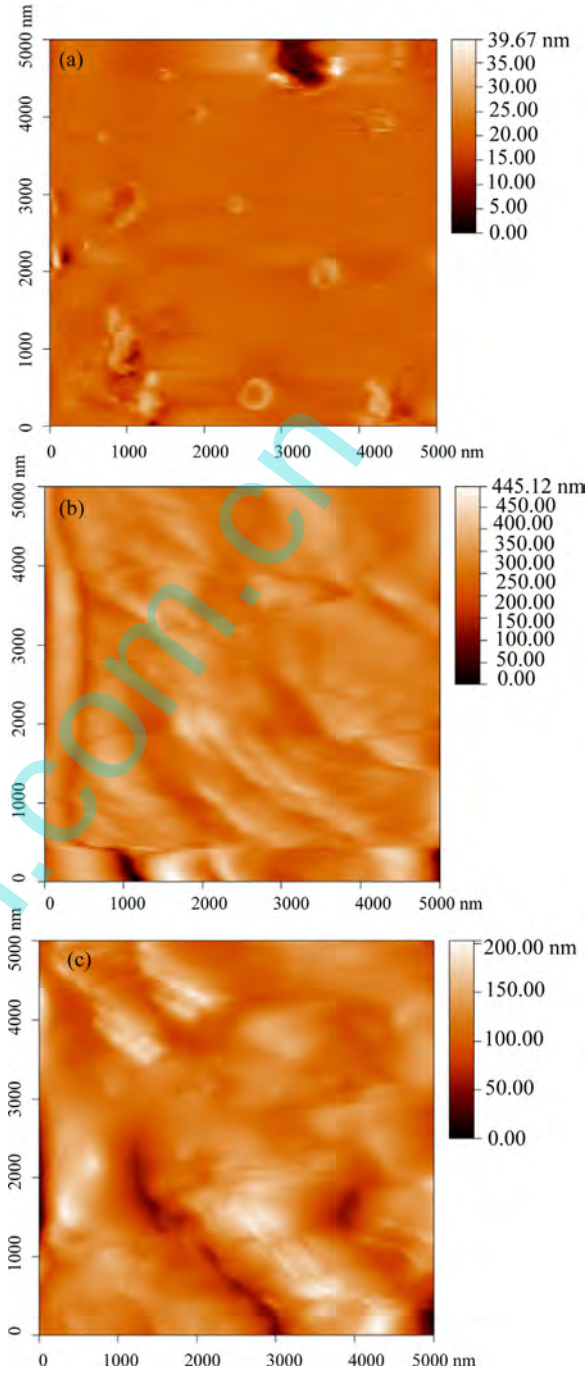

Fig. 5. AFM images of (a) MPTMOS sol–gel, (b) 9.0 wt% GO/MPTMOS sol–gel and (c) AuNPs/9.0 wt% GO/MPTMOS sol–gel films on PET substrate.

3.2. Electrical and humidity-sensing properties of flexible humidity sensors made of AuNPs/GO/MPTMOS sol–gel films

Fig. 7 plots the impedance of the MPTMOS sol–gel, 1.0 wt% GO/MPTMOS sol–gel, AuNPs/1.0 wt% GO/MPTMOS sol–gel and AuNPs/9.0 wt% GO/MPTMOS sol–gel films as functions of relative humidity, and Table 1 summarizes the results concerning sensitivity (defined as the slope of the logarithmic impedance ($\log Z$) versus %RH) and linearity (a correlation coefficient that is defined as the R-squared value of the linear fitting curve from 20 to 90% RH). The measurements were made at 25 °C, an AC voltage of 1 V, and a frequency of 1 kHz. The MPTMOS sol–gel film exhibited only a small change in impedance over the humidity

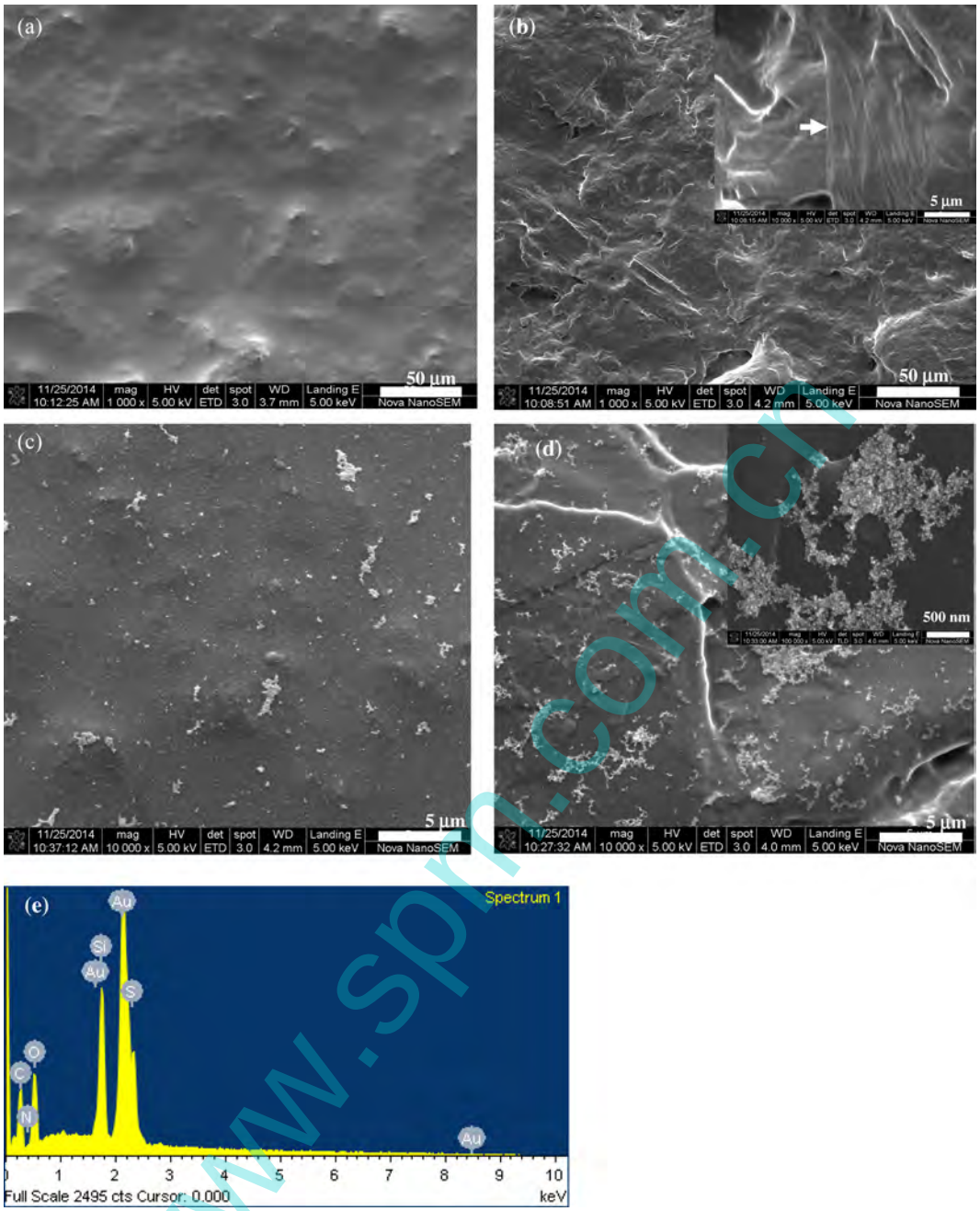

Fig. 6. FE-SEM images of (a) 1.0 wt% GO/MPTMOS sol–gel, (b) 9.0 wt% GO/MPTMOS sol–gel, (c) AuNPs/1.0 wt% GO/MPTMOS sol–gel, (d) AuNPs/9.0 wt% GO/MPTMOS sol–gel films on PET substrate and (e) EDS spectra of AuNPS assembled on the surface of AuNPs/9.0 wt% GO/MPTMOS sol–gel film.

range studied, undoubtedly owing to its hydrophobic property. The impedance of the 1.0 wt% GO/MPTMOS sol–gel film decreased over a wider range of RH (60–90%RH) than did that of the MPTMOS sol–gel film, suggesting that the high hydrophilicity of GO improved the sensitivity of the response. The impedance of the 1.0 wt% GO/MPTMOS sol–gel film was higher than that of the MPTMOS sol–gel film because GO was an electrical insulator. The impedance of AuNPs/GO/MPTMOS sol–gel film was lower than that of the GO/MPTMOS sol–gel film because the aggregated AuNPs formed a new conductive path. Moreover, the impedance of the AuNPs/9.0 wt% GO/MPTMOS sol–gel film was lower than that of the AuNPs/1.0 wt% GO/MPTMOS sol–gel film because as the doping increased and more AuNPs assembled on the naked GO, the conductive path became larger, improving conductivity. The impedance of both AuNPs/1.0 wt% GO/MPTMOS sol–gel and AuNPs/9.0 wt% GO/MPTMOS sol–gel films decreased as the humidity increased in the range 20–90% RH, suggesting higher sensitivity, and improved linearity of the response curve (Table 1). Therefore, both AuNPs/1.0 wt% GO/MPTMOS sol–gel and AuNPs/9.0 wt% GO/MPTMOS sol–gel films were further tested to evaluate their flexibility and stability.

Fig. 8 plots the flexibility-related characteristics of the MPTMOS sol–gel, 9.0 wt% GO/MPTMOS sol–gel and AuNPs/9.0 wt% GO/MPTMOS sol–gel films that were used as humidity sensors. At each bending angle, the sensor was exposed to 60% RH. The deviation (D) of the impedance of the sensors was calculated using the formula $D = (\log Z_{60\%\ RH,\ f} - \log Z_{60\%\ RH,\ b})/\log Z_{60\%\ RH,\ f} \times 100\%)$, where $\log Z_{60\%\ RH,\ f}$ and $\log Z_{60\%\ RH,\ b}$ represent the impedance of the flat and bent flexible humidity sensor at 60% RH, respectively. As described in Section 3.1, the GO was embedded and

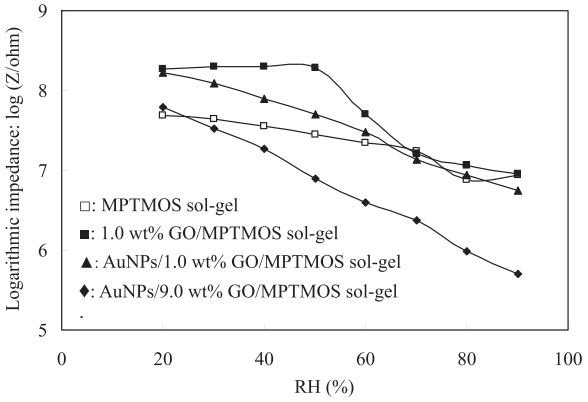

Fig. 7. Impedance versus relative humidity for flexible humidity sensors that were made of MPTMOS sol–gel, 1.0 wt% GO/MPTMOS sol–gel, AuNPs/1.0 wt% GO/MPTMOS sol–gel and AuNPs/9.0 wt% GO/MPTMOS sol–gel films.

Table 1
Sensitivity and linearity of humidity sensors that were made of MPTMOS sol–gel, GO/MPTMOS sol–gel and AuNPs/GO/MPTMOS sol–gel films.

Materials	Sensing curve	
	Sensitivity (log Z/%RH)[a]	Linearity (R^2)[b]
MPTMOS sol–gel	−0.0118	0.9238
1.0 wt% GO/MPTMOS sol–gel	−0.0229	0.8601
AuNPs/1.0 wt% GO/MPTMOS sol–gel	−0.0222	0.9907
AuNPs/9 wt% GO/MPTMOS sol–gel	−0.0281	0.9961

[a] Sensitivity was defined as the slope of the logarithmic impedance versus relative humidity plot in the range 20–90% RH.
[b] Linearity was shown as the correlation coefficient of the logarithmic impedance versus relative humidity plot in the range 20–90% RH.

dispersed in the GO/MPTMOS sol–gel film, and MPTMOS sol–gel wrapping GO was observed. This phenomenon reveals the existence of a strong interface between the GO and the MPTMOS sol–gel matrix. Graphene is known to be highly flexible. Therefore, the 9.0 wt% GO/MPTMOS sol–gel film was more flexible than was the MPTMOS sol–gel film. The assembly of AuNPs on the 9.0 wt% GO/MPTMOS sol–gel film did not obviously decrease its flexibility. Fig. 9 plots the effect of the amount of added GO on the long-term stability of the AuNPs/GO/MPTMOS sol–gel film. The AuNPs/9.0 wt% GO/MPTMOS sol–gel film was more stable than was the AuNPs/1.0 wt% GO/MPTMOS sol–gel film. The flexible humidity sensor that was made of AuNPs/9.0 wt% GO/MPTMOS sol–gel film exhibited the highest sensitivity (0.0281 log Z/%RH), good linearity

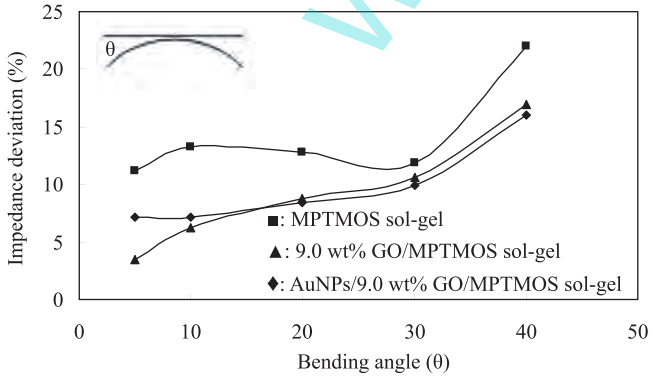

Fig. 8. Flexibility of MPTMOS sol–gel, 9.0 wt% GO/MPTMOS sol–gel and AuNPs/9.0 wt% GO/MPTMOS sol–gel films on PET substrate, measured at 1 V, 1 kHz and 25 °C.

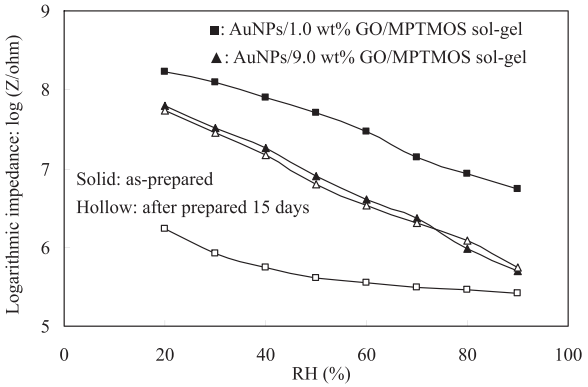

Fig. 9. Long-term stability of AuNPs/1.0 wt% GO/MPTMOS sol–gel and AuNPs/9.0 wt% GO/MPTMOS sol–gel films on PET substrate, measured at 1 V, 1 kHz and 25 °C.

Table 2
Effect of the thickness of the AuNPs/9 wt% GO/MPTMOS sol–gel on the humidity-sensing and flexibility properties.

	Thickness (μm)		
	18.5	71.5	124.7
Sensitivity (log Z/%RH)	−0.0198	−0.0281	−0.0211
Linearity (R^2)	0.9570	0.9961	0.9884
Hysteresis (%RH)	2.8	5	8.3
Response/recovery time (s)	93/102	119/125	163/185
Flexibility (%)	24.2	16.9	13.6

(R^2 = 0.9961), the greatest flexibility (within 16.9% at an angle of up to 40°) and good stability, and so its humidity-sensing properties were investigated. Table 2 summarizes the effect of the thickness of the AuNPs/9.0 wt% GO/MPTMOS sol–gel film on the flexibility and humidity-sensing properties. The 71.5 μm thickness of the AuNPs/9.0 wt% GO/MPTMOS sol–gel film exhibited highest sensitivity and best linearity. The hysteresis, flexibility and response/recovery time of the AuNPs/1.0 wt% GO/MPTMOS sol–gel film increased as the thickness of the AuNPs/1.0 wt% GO/MPTMOS sol–gel film increased.

3.2.1. Humidity-sensing properties

Fig. 10 plots the log-impedance of the flexible humidity sensor versus RH. The measurements were made at 25 °C using an ac voltage of 1 V at 1 kHz. The open symbols in the figure represent measurements made during desiccation, while solid symbols those made during humidification. In the range 20–90% RH, the impedance changed from 10^7 to 10^5 Ω and the curves revealed a satisfactorily linear relationship ($Y = -0.0281X + 8.2721$;

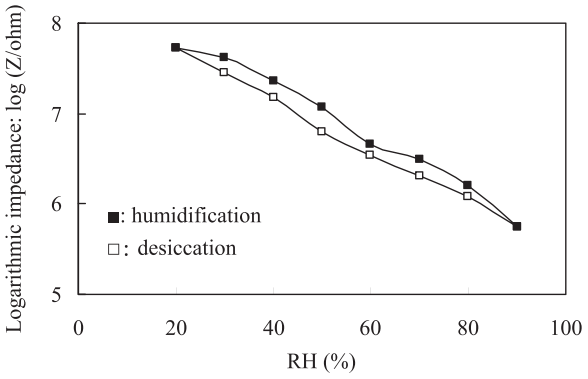

Fig. 10. Impedance versus relative humidity for AuNPs/9.0 wt% GO/MPTMOS sol–gel film on a PET substrate, measured at 1 V, 1 kHz and 25 °C.

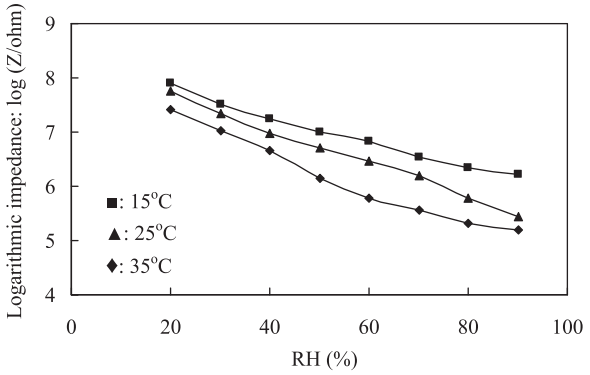

Fig. 11. Impedance versus relative humidity for AuNPs/9.0 wt% GO/MPTMOS sol–gel film on a PET substrate at various temperatures, measured at 1 V and 1 kHz.

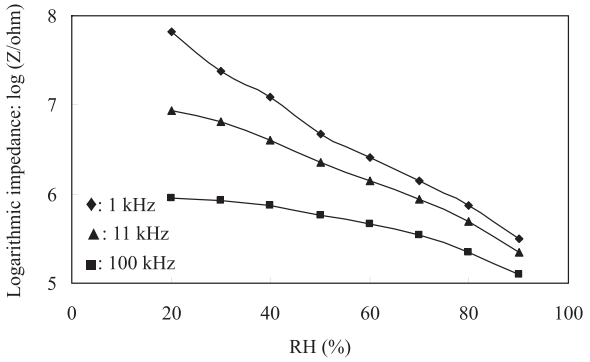

Fig. 12. Impedance versus relative humidity for AuNPs/9.0 wt% GO/MPTMOS sol–gel film on a PET substrate at various frequencies, measured at 1 V and 25 °C.

R^2 = 0.9961) between log-impedance and RH. The hysteresis (between humidification and desiccation, measured over an RH range of 20–90% RH) was less than 5.0% RH. Fig. 11 plots the log-impedance of the humidity sensor versus temperature. As the temperature increased, the RH characteristic curve shifted to lower impedance. The mean temperature coefficient at 15–35 °C was within −1.6% RH/°C over the humidity range 20–90% RH. Fig. 12 plots the log-impedance of the humidity sensor versus measurement frequency at various RH values at a voltage of 1 V. The frequency clearly influenced the humidity-dependence of the impedance of the humidity sensor. The impedance decreased as the frequency increased, and the curve of impedance as a function of RH was most linear at 1 kHz. Fig. 13 plots the response and recovery of the flexible humidity sensor that was measured at 25 °C and 1 kHz. The response time ($T_{res.95\%}$) is defined as the time required

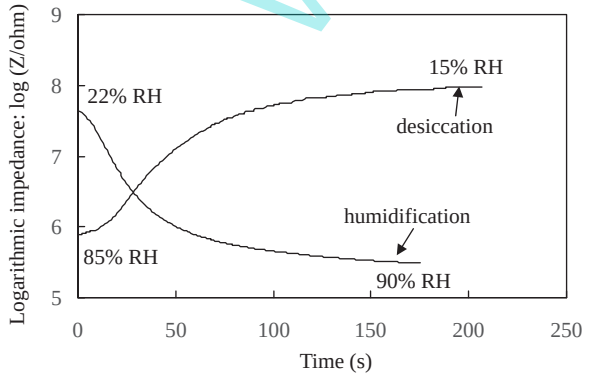

Fig. 13. Response-recovery properties of AuNPs/9.0 wt% GO/MPTMOS sol–gel film on a PET substrate, measured at 1 V, 1 kHz and 25 °C.

Table 3
Flexible humidity sensor performance of this work compared with previous work.

	This work	Previous work [36]
Sensor substrate	PET	PET
Sensing material	AuNPs/9.0 wt% GO/MPTMOS sol–gel	Poly-MMA-MAPTAC
Fabrication method	Self-assembly combining with sol–gel techniques	LBL and peptide chemistry protocol
Working range	20–90% RH	20–90% RH
Sensitivity	−0.0281 log *Z*/%RH	−0.0258 log *Z*/%RH
Linearity	0.9961	0.9910
Hysteresis	5% RH	2% RH
Flexibility	16.9%	0.2%

for the impedance of the sensor to change by 95% of the maximum change following humidification from 22 to 90% RH. The recovery time ($T_{rec.95\%}$) is defined as the time required for the sensor to recover 95% of the maximum change in impedance after desiccation from 85 to 15% RH. The response time ($T_{res.95\%}$) and recovery ($T_{rec.95\%}$) time of the sensor were 119 and 125 s, respectively. The present flexible humidity sensor was compared with that of the sensor that was made of copolymer sensing material as shown in Table 3.

3.3. Sensing mechanism of humidity sensor made of AuNPs/9.0 wt% GO/MPTMOS sol–gel film

Impedance spectroscopy is a powerful method for elucidating the conduction mechanisms of humidity sensors. Therefore, the obtained impedance plots (Fig. 14) were used to elucidate the transport of ions as the mechanism of conduction in the AuNPs/9.0 wt% GO/MPTMOS sol–gel film on PET substrate. The complex impedance spectra of the AuNPs/9.0 wt% GO/MPTMOS sol–gel film at 30 and 80% RH are shown in Fig. 14. The impedance measurements were made at frequencies from 50 Hz to 100 kHz, humidities at 30 and 80% RH, an AC voltage of 1 V and a temperature of 25 °C. At low RH (30% RH), a semicircular plot of film impedance was obtained. As the relative humidity increased to 80% RH, the value of impedance decreased and the semicircular partly disappeared. The shrinking semicircle (at high frequencies) connected with a straight line (at low frequencies). An equivalent circuit of such complex impedance plots is shown in Fig. 14(c). At low relative humidity (<30% RH), the semicircle was modeled as an equivalent circuit of parallel association of resistor (R_f) and capacitor (C_f). At this time the amount of water vapor adsorbed was little, the intrinsic electrons in the AuNPs/9.0 wt% GO/MPTMOS sol–gel film mainly contribute to the conduction. At high relative humidity, the complex impedance plot was modeled as an equivalent circuit of the serial association of resistor (R_f) and the impedance at the electrode/sensing film (Z_i). The plot of impedance entered two regions: a semicircle (at high frequencies) indicated the intrinsic impedance of the AuNPs/9.0 wt% GO/MPTMOS sol–gel film (R_f) and an inclined line (at low frequencies) represented Warburg impedance (Z_i), which was caused by the diffusion of ions (protons (H_3O^+)) across the interface between the electrode and the sensing film [32–35]. Therefore, firstly, upon the adsorption of water, a thin liquid layer formed around the AuNPs/9.0 wt% GO/MPTMOS sol–gel film by capillary condensation or swelling. The conductivity of the sensor was mainly resulted from the intrinsic impedance of the AuNPs/9.0 wt% GO/MPTMOS sol–gel film. Second, as the RH was further increased, water molecules were physisorbed in multilayers on the surface of the AuNPs/9.0 wt% GO/MPTMOS sol–gel film, forming H_3O^+ ions by dissociation. Finally, at the highest RH, the sorbed water acted as a plasticizer, increasing the mobility of the solvated ions (H_3O^+), which dominated the conduction in the sensor. Therefore, based

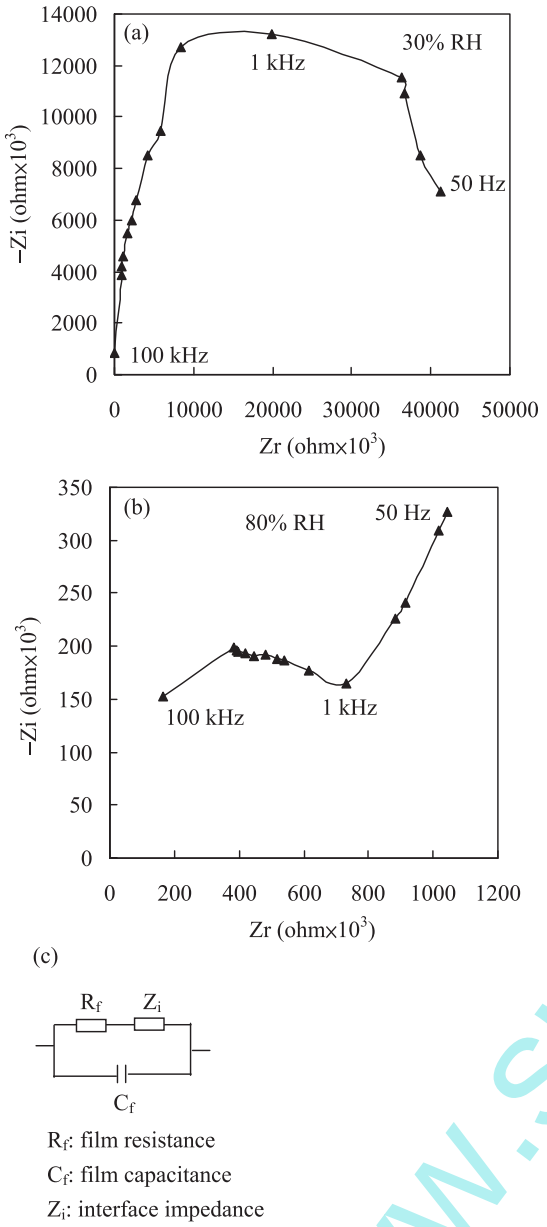

Fig. 14. Complex impedance plots of AuNPs/9.0 wt% GO/MPTMOS sol–gel film on a PET substrate at (a) 30% RH, (b) 80% RH, (c) equivalent circuit of the sensor.

on the complex impedance spectra, the sensing principle of the AuNPs/9.0 wt% GO/MPTMOS sol–gel film was electron and ion conductivity in low and high relative humidity, respectively.

4. Conclusions

The sol–gel process was combined with self-assembly to fabricate a flexible impedance-type humidity sensor that was based on AuNPs/GO/MPTMOS sol–gel film. Thiol-containing silica gel can be anchored onto a gold electrode to form a three-dimensional network, which provides stereo sites for the attachment of GO and AuNPs. Introducing GO effectively increased the flexibility of the AuNPs/GO/MPTMOS sol–gel film. The self-assembly of AuNPs on the silica gel provided the conduction pathways improving the conductivity, and thereby improving the sensitivity and linearity of the sensing film. The flexible humidity sensor that was made of AuNPs/9.0 wt% GO/MPTMOS sol–gel film exhibited good sensitivity and acceptable linearity ($Y = -0.0281X + 8.271$; $R^2 = 0.9961$) between logarithmic impedance ($\log Z$) and RH in the range 20–90% RH, low hysteresis (within 5.0% RH), high flexibility ($D < 16.9\%$), a smaller temperature effect between 15 and 35 °C (−1.6% RH/°C) and good long-term stability. The response time and recovery time of the sensor were 119 and 125 s, respectively. The linearity of the humidity sensor depended on the applied frequency. The plots of the complex impedance of the AuNPs/GO/MPTMOS sol–gel film at various RHs revealed changed from semicircular to a liner with increasing RH. The electron exhibited the domination role in low RH, whereas with increasing RH the ionic contribution became prevalent.

Acknowledgement

The authors thank the Ministry of Science and Technology (grant no. MOST 103-2113-M-034-001) of Taiwan for support.

Appendix A. Supplementary data

Supplementary data associated with this article can be found, in the online version, at http://dx.doi.org/10.1016/j.snb.2015.04.070

References

[1] R. Liang, J. Qiu, P. Cai, A novel amperometric immunosensor based on three-dimensional sol–gel network and nanoparticle self-assemble technique, Anal. Chim. Acta 534 (2005) 223–229.
[2] Bin Hua, W. Chen, J. Zhou, High performance flexible sensor based on inorganic nanomaterials, Sens. Actuators B 176 (2013) 522–533.
[3] T.M. Park, E.I. Iwuoha, M.R. Smyth, R. Freaney, A.J. McShane, Sol–gel based amperometric biosensor incorporating an osmium redox polymer as mediator for detection of L-lactate, Talanta 44 (1997) 973–978.
[4] J. Wang, P.V.A. Pamidi, D.R. Zanette, Self-assembled silica gel networks, J. Am. Chem. Soc. 120 (1998) 5852–5853.
[5] H. Maleki, L. Durães, A. Portugal, An overview on silica aerogels synthesis and different mechanical reinforcing strategies, J. Non-Cryst. Solids 385 (2014) 55–74.
[6] G. Decher, J.D. Hong, J. Schmitt, Buildup of ultrathin multilayer films by a self-assembly process. III. Consecutively alternating adsorption of anionic and cationic polyelectrolytes on charged surface, Thin Solid Films 210 (1992) 831–835.
[7] G. Decher, Fuzzy nanoassemblies: toward layered polymeric multicomposites, Science 277 (1997) 1232–1237.
[8] A. Taheri, M. Noroozifar, M. Khorasani-Motlagh, Investigation of a new electrochemical cyanide sensor based on Ag nanoparticles embedded in a three-dimensional sol–gel, J. Electroanal. Chem. 628 (2009) 48–54.
[9] S. Houa, Z. Oub, Q. Chenc, B. Wu, Amperometric acetylcholine biosensor based on self-assembly of gold nanoparticles and acetylcholinesterase on the sol–gel/multi-walled carbon nanotubes/choline oxidase composite-modified platinum electrode, Biosens. Bioelectron. 33 (2012) 44–49.
[10] S. Guo, E. Wang, Synthesis and electrochemical applications of gold nanoparticles, Anal. Chim. Acta 598 (2007) 181–192.
[11] K.S. Novoselov, A.K. Geim, S.V. Morozov, D. Jiang, Y. Zhang, S.V. Dubonos, I.V. Grigorieva, A.A. Firsov, Electric field effect in atomically thin carbon films, Science 306 (2004) 666–669.
[12] R.F. Service, Carbon sheets an atom thick give rise to graphene dreams, Science 324 (2009) 875–877.
[13] Y.Y. Shao, J. Wang, H. Wu, J. Liu, I.A. Aksay, Y.H. Lin, Graphene based electrochemical sensors and biosensors: a review, Electroanalysis 22 (2010) 1027.
[14] W.S. Hummers, R.E. Offeman, Preparation of graphitic oxide, J. Am. Chem. Soc. 80 (1958) 1339.
[15] A. Lerf, H. He, M. Forster, J. Kilnowski, Structure of graphite oxide revisited, J. Phys. Chem. B 102 (1998) 4477–4482.
[16] S. Stankovich, D.A. Dikin, R.D. Piner, K.A. Kohlhaas, A. Kleinhammes, Y. Jia, Y. Wu, S.B.T. Nguyen, R.S. Ruoff, Synthesis of graphene-based nanosheets via chemical reduction of exfoliated graphene oxide, Carbon 45 (2007) 1558–1565.
[17] W. Gao, L.B. Alemany, L. Ci, P.M. Ajayan, New insights into the structure and reduction of graphite oxide, Nat. Chem. 1 (2009) 403–408.
[18] J. Cao, F. Liu, N. Ma, Z. Wang, X. Zhang, Environment-friendly method to produce graphene that employs vitamin C and amino acid, Chem. Mater. 22 (2010) 2213–2218.
[19] S.F. Pei, H.M. Cheng, The reduction of graphene oxide, Carbon 50 (2012) 3210–3228.
[20] G. Lu, L.E. Ocola, J. Chen, Gas detection using low-temperature reduced graphene oxide sheets, Appl. Phys. Lett. 94 (2009) 083111–83113.
[21] Y. Yao, X.D. Chen, H.H. Guo, Z.Q. Wu, Graphene oxide thin film coated quartz crystal microbalance for humidity detection, Appl. Surf. Sci. 257 (2011) 7778–7782.

[22] L. Guo, H.B. Jiang, R.Q. Shao, Y.L. Zhang, S.Y. Xie, J.N. Wanf, X.B. Li, F. Jiang, Q.D. Chen, T. Zhang, H.B. Sun, Two-beam-layser interference mediated reduction, patterning and nanostructuring of graphene oxide for the production of a flexible humidity sensing device, Carbon 50 (2012) 1667–1673.
[23] Q. Huang, D. Zeng, S. Tian, C. Xie, Synthesis of defect and its application for room temperature humidity sensing, Mater. Lett. 83 (2012) 76–79.
[24] Y. Yao, X.D. Chen, H.H. Guo, Z.Q. Wu, X.Y. Li, Humidity sensing behaviors of graphene oxide-silicon bi-layer flexible structure, Sens. Actuators B 161 (2012) 1053–1058.
[25] H.D. Hill, C.A. Mirkin, The bio-barcode assay for the detection of protein and nucleic acid targets using DDT-induced ligand exchange, Nat. Protoc. 1 (2006) 324–336.
[26] P.G. Su, I.C. Chen, R.J. Wu, Use of poly(2-acrylamido-2-methylpropane sulfonate) modified with tetraethyl orthosilicate as sensing material for measurement of humidity, Anal. Chim. Acta 449 (2001) 103–109.
[27] F. Wu, Z. Hu, J. Xu, Y. Tian, L. Wang, Y. Xian, L. Jin, Immobilization of horseradish peroxidase on self-assembled (3-mercaptopropyl)trimethoxysilane film: characterization, direct electrochemistry, redox thermodynamics and biosensing, Electrochim. Acta 53 (2008) 8238–8244.
[28] S. Bharathi, M. Nogami, S. Ikeda, Novel electrochemical interfaces with a tunable kinetic barrier by self-assembling organically modified silica gel and gold nanoparticles, Langmuir 17 (2001) 1–4.
[29] S.K. Ghost, T. Pal, Interparticle coupling effect on the surface plasmon resonance of gold nanoparticles: from theory to applications, Chem. Rev. 107 (2007) 4797–4862.
[30] A.N. Shipway, M. Lahav, R. Gabai, I. Willner, Investigations into the electrostatically induced aggregation of Au nanoparticles, Langmuir 16 (2000) 8789–8795.
[31] L.R. Allain, K. Sorasaenee, Z. Xue, Doped thin-film sensors via a sol–gel process for high-acidity determination, Anal. Chem. 69 (1997) 3076–3080.
[32] C.D. Feng, S.L. Sun, H. Wang, C.U. Segre, J.R. Stetter, Humidity sensing properties of Nafion and sol–gel derived SiO_2/Nafion composite thin films, Sens. Actuators B 40 (1997) 217–222.
[33] G. Casalbore-Miceli, M.J. Yang, N. Camaioni, C.M. Mari, Y. Li, H. Sun, M. Ling, Investigations on the ion transport mechanism in conduction polymer films, Solid State Ionics 131 (2000) 311–321.
[34] J. Wang, Q. Lin, T. Zhang, R. Zhou, B. Xu, Humidity sensor based on composite material of nano-$BaTiO_3$ and polymer RMX, Sens. Actuators B 81 (2002) 248–253.
[35] J. Wang, B.K. Xu, S.P. Ruan, S.P. Wang, Preparation and electrical properties of humidity sensing films of $BaTiO_3$/polystrene sulfonic sodium, Mater. Chem. Phys. 78 (2003) 746–750.
[36] P.G. Su, H.C. Hsu, C.Y. Liu, Layer-by-layer anchoring of copolymer of methyl methacrylate and[3-(methacrylamino)propyl] trimethyl ammonium chloride to gold surface on flexible substrate for sensing humidity, Sens. Actuators B 178 (2013) 289–295.

Biographies

Pi-Guey Su is currently a Professor in Department of Chemistry at Chinese Culture University. He received his BS degree from Soochow University in Chemistry in 1993 and PhD degree in Chemistry from National Tsing Hua University in 1998. He worked as a Researcher in Industrial Technology Research Institute, Taiwan, from 1998 to 2002. He joined as an Assistant Professor in the General Education Center, Chungchou Institute of Technology from 2003 to 2005. He worked as an Assistant Professor in Department of Chemistry at Chinese Culture University from 2005 to 2007. He worked as an associate professor in Department of Chemistry at Chinese Culture University from 2007 to 2010. His fields of interests are chemical sensors, gas and humidity sensing materials and humidity standard technology.

Wei-Luen Shiu received a BS degree in chemistry from Chinese Culture University in 2012. She entered the MS course of chemistry at Chinese Culture University in 2012. Her main areas of interest are gas sensing materials.

Meng-Shian Tsai received a BS degree in chemistry from National Sun Yat-Sen University in 2010. He entered the MS course of chemistry at Chinese Culture University in 2010. His main areas of interest are fabrication of biosensors and electrochemical.